

The rms peculiar velocity of galaxy clusters for different cluster masses and radii

Ivan Suhonenko and Mirt Gramann

Tartu Observatory, Tõravere 61602, Estonia

26 October 2018

ABSTRACT

We investigate the rms peculiar velocity of galaxy clusters in the Lambda cold dark matter (Λ CDM) and tau cold dark matter (τ CDM) cosmological models using N-body simulations. Cluster velocities for different cluster masses and radii are examined. To identify clusters in the simulations we use two methods: the standard friends-of-friends (FOF) method and the method, where the clusters are defined as the maxima of the density field smoothed on the scale $R \sim 1h^{-1}$ Mpc (DENSMAX). If we use the DENSMAX method, the size of the selected clusters is similar for all clusters. We find that the rms velocity of clusters defined with the DENSMAX method is almost independent of the cluster density and similar to the linear theory expectations. The rms velocity of FOF clusters decreases with the cluster mass and radius. In the Λ CDM model, the rms peculiar velocity of massive clusters with an intercluster separation $d_{cl} = 50h^{-1}$ Mpc is $\approx 15\%$ smaller than the rms velocity of the clusters with a separation $d_{cl} = 10h^{-1}$ Mpc.

Key words: galaxies: clusters: general – cosmology: theory – dark matter – large-scale structure of Universe.

1 INTRODUCTION

One of the interesting unknowns in cosmology is the large-scale peculiar velocity field in the Universe. The peculiar velocity field can be studied by using galaxies or clusters of galaxies. However, there are some advantages in studying the peculiar velocity field by using galaxy clusters. One of these advantages comes from the fact that, on scales probed by galaxy clusters, velocity fluctuations are largely in the quasi-linear regime and close to the initial state from which large scale structures developed. In addition, peculiar velocities of clusters can be determined more accurately than peculiar velocities of galaxies since the distance to each cluster can be obtained from a large number of member galaxies, thus considerably reducing the velocity uncertainties of clusters. Cluster motions could therefore provide an important tool in probing the large-scale peculiar velocity field.

Peculiar velocities of clusters of galaxies have been studied in several papers (e.g. Bahcall, Gramann & Cen 1994; Lauer & Postman 1994; Bahcall & Oh 1996; Moscardini et al. 1996; Borgani et al. 1997; Watkins 1997; Dale et al. 1999; Hudson et al. 1999; Borgani et al. 2000; Colless et al. 2001). Watkins (1997) developed a likelihood method for estimating the rms peculiar velocity of clusters from line-of sight velocity measurements. This method was applied to two observed samples of cluster peculiar velocities: the SCI sample (Giovanelli et al. 1997) and a subsample of the Mark III

catalogue (Willick et al. 1997). Watkins (1997) found that the rms one-dimensional cluster peculiar velocity is 256_{-75}^{+106} km s $^{-1}$, which corresponds to the three-dimensional rms velocity 459_{-130}^{+184} km s $^{-1}$. Dale et al. (1999) obtained Tully-Fisher peculiar velocities for 52 Abell clusters distributed over the whole of the sky between ~ 50 and $\sim 200h^{-1}$ Mpc. They found that the rms one-dimensional cluster peculiar velocity is 341 ± 93 km s $^{-1}$, which corresponds to the three-dimensional rms velocity 591 ± 161 km s $^{-1}$.

Radial peculiar velocities of clusters can be determined to large distances by measuring the Sunyaev-Zeldovich (1980) (SZ) effect. Rephaeli & Lahav (1991) made one of the first estimates of the possibility of measuring the peculiar velocities by using the SZ effect for a selected sample of galaxy clusters. However, most convincing measurements for individual clusters have been done only recently, using the new generation of sensitive bolometers (Holzapfel et al. 1997; Lamarre et al. 1998). The accuracy of SZ measurements for determining peculiar velocities of clusters have been studied in several papers (Haehnelt & Tegmark 1996; Aghanim, Gorski & Puget 2001; Diego et al. 2002; Holder 2002; Nagaia, Kravtsov & Kosowsky 2002). With μK sensitivity on arcminute scales at several frequencies it will be possible to measure peculiar velocities to an accuracy of ~ 130 km s $^{-1}$.

In this paper we study the rms peculiar velocity of clusters, v_{rms} , in different cosmological models assuming that the initial density fluctuation field is a Gaussian field. To in-

vestigate the nonlinear regime, we use N-body simulations. We examine cluster peculiar velocities for different cluster masses. Do cluster velocities depend on their masses? The rms peculiar velocity of peaks in the initial Gaussian field does not depend on the height of peaks (Bardeen et al. 1986). However, as an initially Gaussian density field evolves gravitationally in the nonlinear regime, it becomes non-Gaussian.

The evolution of peculiar velocities of galaxy clusters in different N-body models with an initially Gaussian density field has been examined in several papers (e.g. Bahcall, Gramann, Cen 1994; Croft & Efstathiou 1994; Suhonenko & Gramann 1999, Colberg et al 2000; Sheth & Diaferio 2001). Groth & Efstathiou (1994) studied the cluster peculiar velocities for two different cluster richesses, described by the mean intercluster separations $d_{cl} = 30h^{-1}$ Mpc and $d_{cl} = 55h^{-1}$ Mpc. They found that the peculiar velocity distributions are almost independent of cluster richness. Sheth & Diaferio (2001) studied rms peculiar velocity of clusters for different masses and found that in N-body simulations the rms velocity of clusters depends weakly on cluster mass, with a small trend that for more massive clusters the rms peculiar velocity decreases. On the other hand, Suhonenko & Gramann (1999) investigated the properties of clusters using N-body simulations and found that the rms peculiar velocities of clusters increase with cluster richness.

In this paper we study the dependence of v_{rms} on cluster masses in more detail. We also examine the rms peculiar velocities of clusters for different cluster radii. We use the N-body simulations published by the Virgo Consortium and described in detail by Jenkins et al. (1998). These simulations were carried out using a parallel, adaptive particle-particle/particle-mesh (AP³M) code (Couchman, Thomas & Pearce 1995; Pearce & Couchman 1997). In this paper we analyze the velocities in the Λ CDM and τ CDM model (see Jenkins et al. (1998) and Section 2 for the description of the cosmological parameters in these models). We also follow the evolution of particles in a similar Λ CDM model with the same cosmological parameters but using a particle-mesh (PM) code. In this PM code we use a traditional two-point finite-difference approximation to calculate the forces on the grid. We also examine the shifted-mesh scheme (see eq. (13) below) and show that this scheme artificially boosts the velocities of clusters.

To identify clusters in the simulations we use two methods: the standard friends-of-friends (FOF) method and the method, where the clusters are defined as the maxima of the density field smoothed on the scale $R \sim 1h^{-1}$ Mpc (DENSMAX). To determine the velocity of DENSMAX clusters, we use the same smoothing scale as for the density field. The velocity of FOF clusters is defined to be the mean velocity of all the particles in the cluster.

This paper is organized as follows. In Section 2 we describe the cosmological models, N-body simulations and cluster selection algorithms used. We also examine the linear theory predictions for the peculiar velocities of peaks in the Gaussian field. In Section 3 we examine the rms peculiar velocity of clusters for different cluster masses and radii, and compare the cluster velocities with the linear theory predictions. In Section 4 we briefly discuss the effect of the shifted-mesh scheme on the cluster velocities. A summary and discussion are presented in Section 5.

2 MODELS

2.1 Simulations

We analyze peculiar velocities in N-body simulations carried out by the Virgo consortium for two cosmological models, Λ CDM ($\Omega_0 = 0.3$, $\Lambda = 0.7$) and τ CDM ($\Omega_0 = 1$) as described by Jenkins et al. (1998). In these cold dark matter (CDM) models the power spectrum of the initial conditions was chosen to be in the form given by Bond & Efstathiou (1984),

$$P(k) = \frac{Ak}{[1 + (aq + (bq)^{3/2} + (cq)^2)^\nu]^{2/\nu}}, \quad (1)$$

where $q = k/\Gamma$, $a = 6.4h^{-1}$ Mpc, $b = 3h^{-1}$ Mpc, $c = 1.7h^{-1}$ Mpc, $\nu = 1.13$ and $\Gamma = 0.21$. The normalization constant, A , was chosen by fixing the value of σ_8 (the linearly extrapolated mass fluctuation in spheres of radius $8h^{-1}$ Mpc); $\sigma_8 = 0.9$ and $\sigma_8 = 0.51$ for the Λ CDM and τ CDM model, respectively.

We investigated the linear theory predictions for peculiar velocities of peaks in the Λ CDM and τ CDM model. The linear rms velocity fluctuation on a given scale R can be expressed as

$$\sigma_v(R) = H_0 f(\Omega_0) \sigma_{-1}(R), \quad (2)$$

where the spectral moments σ_j are defined for any integer j by

$$\sigma_j^2 = \frac{1}{2\pi^2} \int P(k) W^2(kR) k^{2j+2} dk, \quad (3)$$

$W(kR)$ is a window function and $f(\Omega_0)$ is the dimensionless growth rate. The function $f(\Omega_0) = 0.51$ and $f(\Omega_0) = 1.0$ in the Λ CDM and τ CDM model, respectively. (We note that the approximation $f(\Omega_0) = \Omega_0^{0.6}$ underestimates the dimensionless growth rate by $\sim 5\%$ in the flat $\Omega_0 = 0.3$ model).

Bardeen et al. (1986) showed that in the linear approximation the rms peculiar velocity at peaks of the smoothed density field differs systematically from $\sigma_v(R)$, and can be expressed as

$$\sigma_p(R) = \sigma_v(R) \sqrt{1 - \sigma_0^4/\sigma_1^2 \sigma_{-1}^2}. \quad (4)$$

In this approximation, the rms velocities of peaks do not depend on the height of the peaks.

Fig. 1 shows the rms peculiar velocity of peaks, $\sigma_p(R)$, for the Λ CDM and τ CDM model. We have used the top-hat window function. For comparison, we show also the rms peculiar velocity $\sigma_v(R)$ for the same models. For the radius $R = 1h^{-1}$ Mpc, $\sigma_p = 509$ km/s and $\sigma_p = 562$ km/s in the Λ CDM and τ CDM models, respectively. At this radius, σ_p is lower than σ_v about ~ 2 per cent for the models studied. On larger scales, the difference between σ_p and σ_v increases.

Next we study peculiar velocities in N-body simulations. The Virgo simulations were created using a parallel adaptive particle-particle/particle-mesh (AP³M) code as described by Couchman, Thomas & Pearce (1995) and Pearce & Couchman (1997). It supplements the standard P³M algorithm (Efstathiou et al. 1985) by recursively placing higher resolution meshes, ‘refinements’, in heavily clustered regions. The Virgo simulations were done on two large Cray T3D parallel supercomputers at the Edinburgh Parallel Computing Center and at the Computing Center of the Max Plank Soci-

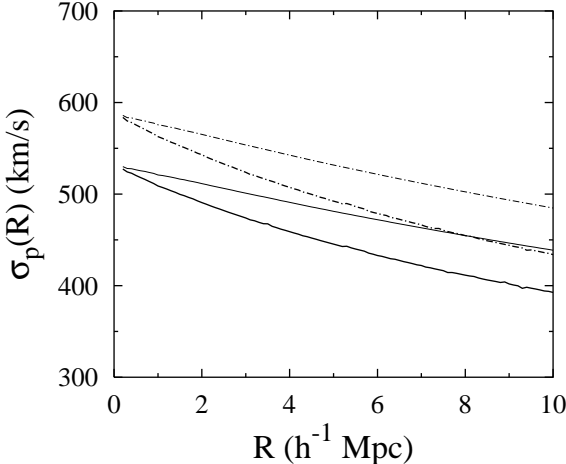


Figure 1. The rms peculiar velocity of peaks, $\sigma_p(R)$, in the Λ CDM model with $\Omega_0 = 0.3$ and $\sigma_8 = 0.9$ (heavy solid line) and in the τ CDM model with $\Omega_0 = 1.0$ and $\sigma_8 = 0.51$ (heavy dot-dashed line). The light curves show the corresponding rms peculiar velocity $\sigma_v(R)$ for the same models.

ety in Garching. These simulations are publicly available at <http://www.mpa-garching.mpg.de/Virgo/virgoproject.html>.

In the simulations used here, the evolution of particles was followed in the comoving box of size $L = 239.5h^{-1}$ Mpc. The number of particles was $N_p = 256^3$. Therefore, the mean particle separation $\lambda_p = L/N_p^{1/3} = 0.9355h^{-1}$ Mpc. The mass of the particle $m_p = \rho_b \lambda_p^3 = 6.82 \times 10^{10} h^{-1} M_\odot$ and $m_p = 2.27 \times 10^{11} h^{-1} M_\odot$ in the Λ CDM and τ CDM models, respectively (here ρ_b is the mean background density). The gravitational softening length is $r_{soft} = 25h^{-1}$ kpc and $r_{soft} = 36h^{-1}$ kpc, respectively (see Jenkins et al. (1998) for a detailed description of the force calculation scheme used in the Virgo simulations). We denote the Virgo Λ CDM and τ CDM models as the model Λ CDM1 and τ CDM.

We also investigated the evolution of 256^3 particles on a 256^3 grid using a particle-mesh (PM) code described by Gramann (1988) and Suhhonenko & Gramann (1999). The PM code achieves the force resolution close to the mean particle separation λ_p . The PM method is discussed in detail by Hockney & Eastwood (1981) and Efstathiou et al. (1985). The cosmological parameters for this PM simulation were chosen similar to the Λ CDM1 model. We chose the flat $\Omega_0 = 0.3$ model and used the initial power spectrum $P(k)$ given in eq. (1) (with $\sigma_8 = 0.9$). The comoving box size was $L = 239.5h^{-1}$ Mpc. Therefore, the mean particle separation, λ_p , and the mass of the particle, m_p , in this model are the same as used in the Λ CDM1 model. We denote this model as the Λ CDM2 model.

We examined the rms velocity of particles in the simulations studied. In the Λ CDM1 and τ CDM models, the rms velocity of particles was 648 km s^{-1} and 636 km s^{-1} , respectively. In the Λ CDM2 model, the rms velocity was 575 km s^{-1} . Due to the small-scale smoothing inherent to the PM method, the intrinsic velocity dispersions of clusters in the Λ CDM2 model are smaller than in the Λ CDM1 model. The velocity field of clusters in these models is expected to be similar.

In the Λ CDM2 model we used the traditional two-point

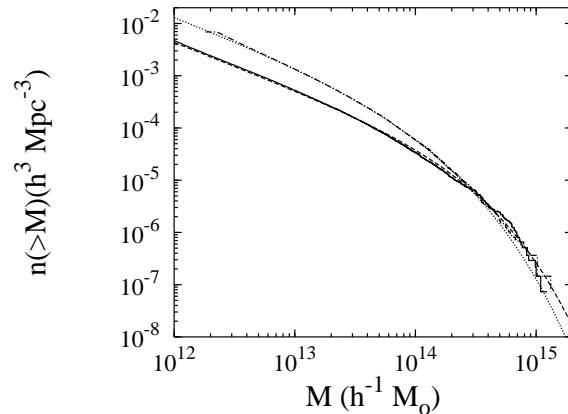


Figure 2. The cluster mass function in the Virgo Λ CDM model for the parameter $b = 0.164$ (solid line) and in the τ CDM model for $b = 0.2$ (dot-dashed line). For comparison we show the fitting formulae given by Jenkins et al. (2001) for the mass function in the Λ CDM (dashed line) and in the τ CDM model (dotted line).

approximation to calculate the acceleration on the grid. We also studied the evolution of particles using a PM code with the shifted-mesh scheme. The effect of the shifted-mesh scheme on the cluster velocities is discussed in Section 4.

2.2 Selection of clusters

We used two different algorithms to identify clusters in simulations: the standard friends-of-friends (FOF) algorithm, and the algorithm, where clusters are defined as maxima of the density field smoothed on the scale $R \sim 1h^{-1}$ Mpc (DENSMAX).

The friends-of-friends group finder algorithm was applied using the program suite developed by the cosmology group in the University of Washington. These programs are available at <http://www-hpcc.astro.washington.edu>.

The FOF cluster finder depends on one parameter b , which defines the linking length as $b\lambda_p$. The conventional choice for this parameter is $b = 0.2$ (see e.g. Götz, Huchra & Brandenberger 1998; Jenkins et al. 2001). In this paper we also define clusters by using the value $b = 0.2$. We also study velocities of the clusters defined by the parameters $b = 0.15$ and $b = 0.3$. In the limit of very large numbers of particles per object, FOF approximately selects the matter enclosed by an isodensity contour at $1/b^3$.

To test our FOF output data, we found the mass function of clusters in the Virgo simulations. The cluster mass function in these simulations has been studied in detail by Jenkins et al. (2001). Fig. 2 shows the mass function of clusters determined for $b = 0.164$ in the Λ CDM model and for $b = 0.2$ in the τ CDM model. For comparison we show the mass functions given by the approximations obtained by Jenkins et al. (2001) (eq. (B2) and (B1) for the Λ CDM and τ CDM model, respectively). Jenkins et al. (2001) studied the mass function at the high mass end up to the point where the predicted Poisson abundance errors reach 10%. In the simulations studied here, this limit is reached when the number density of clusters is $n = 7.3 \times 10^{-6} h^3 \text{ Mpc}^{-3}$. Fig. 2 shows that if n is larger than this value, the agree-

ment between our results and these obtained by Jenkins et al. (2001) is very good.

We studied clusters that contained at least ten particles. The three-dimensional velocity of each cluster was defined as

$$\vec{v}_{cl} = \frac{1}{N_p} \sum_{i=1}^{N_p} \vec{v}_i, \quad (5)$$

where N_p is the number of particles in the cluster and \vec{v}_i is the velocity of the particle i in the cluster. To characterize the size of the cluster, we use the effective radius defined as

$$R_{eff} = \frac{1}{N_p} \sum_{i=1}^{N_p} [(x_i - \bar{x})^2 + (y_i - \bar{y})^2 + (z_i - \bar{z})^2]^{1/2}, \quad (6)$$

where x_i, y_i, z_i are the particle coordinates in the cluster and $(\bar{x}, \bar{y}, \bar{z})$ are the coordinates of the cluster centre. If we use the FOF method, the mean size for the high-mass clusters is larger than the mean size for the low-mass clusters.

We also selected clusters using the DENS MAX method. In this case clusters were identified in the simulations as maxima of the density field that was determined on a 256^3 grid using the cloud-in-cell (CIC) scheme. To determine peculiar velocities of clusters, v_{cl} , we calculated the peculiar velocity field on a 256^3 grid using the CIC-scheme, and found peculiar velocities at the grid points where the clusters had been identified. If we use the DENS MAX method, the size of the selected clusters is similar for all clusters, given by the cell size, λ_g . In our case, the cell size $\lambda_g = 0.9355 h^{-1}$ Mpc.

To determine the rms peculiar velocities of clusters, we used the equation

$$v_{rms}^2 = v_s^2 + v_L^2 = \frac{1}{N_{cl}} \sum_{i=1}^{N_{cl}} v_{cli}^2 + v_L^2, \quad (7)$$

where the parameter v_s describes the dispersion of cluster velocities, v_{cli} , derived from simulation and the parameter v_L is the linear contribution from velocity fluctuations on scales greater than the size of the simulation box L and is given by

$$v_L^2 = \frac{f^2(\Omega_0) H_0^2}{2\pi^2} \int_0^{2\pi/L} P(k) dk. \quad (8)$$

N_{cl} is the number of clusters studied. By using eq. (4), the linear rms peculiar velocity of peaks can be written as

$$\sigma_p^2(R) = \sigma_v^2(R) - H_0^2 f^2(\Omega_0) \frac{\sigma_0^4(R)}{\sigma_1^2(R)}. \quad (9)$$

The second term in this expression is not sensitive to the amplitude of large-scale fluctuations at wavenumbers $k < 2\pi/L$. Therefore, the linear rms velocity of peaks can be expressed as

$$\sigma_p^2(R) = \sigma_p'^2(R) + v_L^2, \quad (10)$$

where $\sigma_p'(R)$ is determined by the power spectrum at wavenumbers $k > 2\pi/L$ and v_L is given by eq. (8). For Λ CDM and τ CDM models, we found that $v_L = 220 \text{ km s}^{-1}$ and $v_L = 245 \text{ km s}^{-1}$, respectively.

If the one-dimensional velocities of clusters, v_{xi} , follow

Table 1. The number of clusters, N_{cl} , in different density and mass intervals. N_{cl} for different density intervals is given for the clusters selected with the DENS MAX method. N_{cl} for different mass intervals is given for the clusters determined with the FOF method with $b = 0.2$.

ρ/ρ_b	N_{cl} Λ CDM1	N_{cl} τ CDM	N_{cl} Λ CDM2
1 – 5	148496	169774	103757
5 – 10	29265	35753	17369
10 – 50	31294	34705	18314
50 – 100	5246	4015	3372
100 – 500	4253	1762	2619
500 – 1000	298	22	107
1000 – 5000	78	0	8

M ($h^{-1} M_\odot$)	N_{cl} Λ CDM1	N_{cl} τ CDM	N_{cl} Λ CDM2
$5 \times 10^{11} - 10^{12}$	36227	0	27310
$10^{12} - 5 \times 10^{12}$	51841	57460	15820
$5 \times 10^{12} - 10^{13}$	7326	19298	3204
$10^{13} - 5 \times 10^{13}$	6542	15489	4225
$5 \times 10^{13} - 10^{14}$	856	1644	659
$10^{14} - 5 \times 10^{14}$	511	789	507
$5 \times 10^{14} - 10^{15}$	38	18	24
$10^{15} - 5 \times 10^{15}$	4	5	3

a Gaussian distribution with a mean $\bar{v}_x = 0$ and a dispersion σ^2 , then the sum

$$\chi^2 = \frac{1}{\sigma^2} \sum_{i=1}^{N_{cl}} v_{cli}^2 \quad (11)$$

is distributed as a χ^2 distribution with the number of degrees of freedom $\nu = 3N_{cl}$. In this case, the rms error for the variable v_{rms}^2 can be determined as

$$\Delta v_{rms}^2 = \sqrt{\frac{2}{3N_{cl}}} v_s^2. \quad (12)$$

As a first step, the one-dimensional distribution of cluster velocities can be approximated as a Gaussian distribution (see e.g. Bahcall, Gramann, Cen (1994) for the study of the velocity distribution of clusters in different cosmological models). We used eq. (12) to estimate the error bars for the rms velocities of clusters.

3 RESULTS

First, we investigated the rms velocity of clusters in different density and mass intervals. The results are presented in Fig. 3. The rms velocities are shown for the intervals, where the number of clusters is $N_{cl} > 10$.

The clusters defined with the DENS MAX method were divided into subgroups according to their density. We studied the rms velocity of clusters in seven subgroups, where the density ρ/ρ_b was in the range 1 – 5, 5 – 10, 10 – 50, ..., 1000 – 5000. Table 1 shows the number of clusters and the upper right panel in Fig. 3 shows the rms velocity of clusters in different density intervals. We see that the rms velocities of clusters in the Λ CDM1 and Λ CDM2 models are similar. In the models studied, the rms velocity of clusters is almost

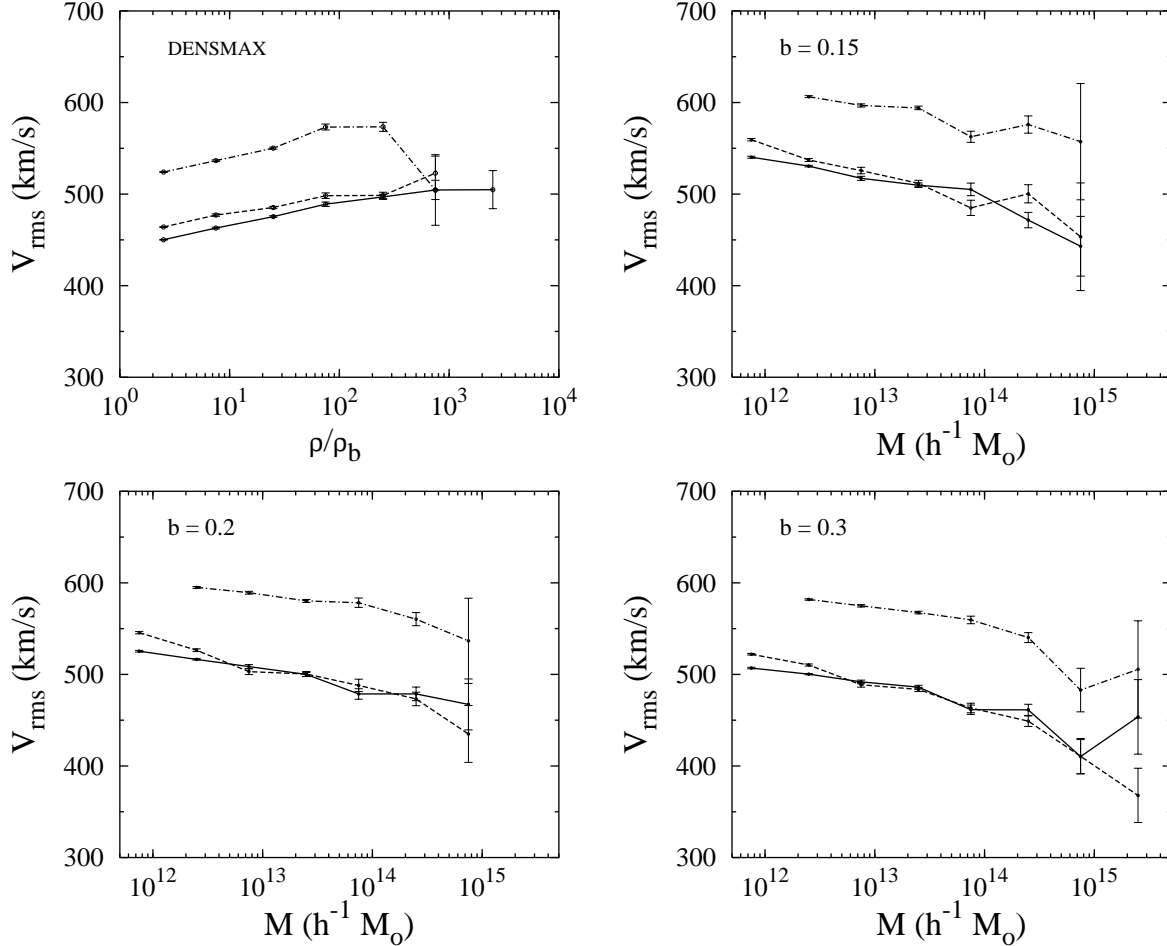


Figure 3. The rms peculiar velocities of clusters for different densities and masses in the Λ CDM1 model (solid lines), τ CDM model (dot-dashed lines) and in the Λ CDM2 model (dashed lines). The upper left panel shows the results for the clusters defined by the DENS MAX method and the lower left panel shows the results for the clusters selected by the FOF method with $b = 0.2$. The right panels show the rms velocities of clusters defined by the FOF method with $b = 0.15$ and $b = 0.3$, respectively.

independent of the density. The rms velocity somewhat increases at smaller densities. However, this increase is small (≈ 10 per cent). For the range $\rho/\rho_b = 100 - 500$, the rms velocity is 505 km s^{-1} and 570 km s^{-1} in the Λ CDM1 and τ CDM models, respectively. These values are similar to the linear theory expectations. At the radius $R = 1h^{-1} \text{ Mpc}$, the rms peculiar velocity of peaks $\sigma_p = 509 \text{ km s}^{-1}$ and 562 km s^{-1} in the Λ CDM1 and τ CDM models, respectively. The rms velocity for the low-density clusters is somewhat smaller than predicted by the linear theory.

The clusters determined with the FOF method were divided into subgroups according to their mass. We studied the rms velocity of clusters in eight subgroups, where the mass was in the range $(5 \times 10^{11} - 10^{12})h^{-1} M_\odot, \dots, (10^{15} - 5 \times 10^{15})h^{-1} M_\odot$. Table 3 shows the number of clusters and Fig. 3 demonstrates the rms peculiar velocity of clusters in different mass intervals. The lower left panel in Fig. 3 shows the results for the clusters determined by $b = 0.2$. The right panels show the rms velocities of clusters defined by $b = 0.15$ and $b = 0.3$.

We see that in the Λ CDM1 and Λ CDM2 models the rms velocities are similar. The rms velocity of FOF clusters decreases with cluster mass. The rms velocity of massive

FOF clusters is smaller than the rms velocity of high-density clusters determined with the DENS MAX method. In the Λ CDM model for $b = 0.2$, the rms velocity of clusters is 525 km s^{-1} in the mass interval $(5 \times 10^{11} - 10^{12})h^{-1} M_\odot$ and 430 km s^{-1} in the mass interval $(10^{15} - 5 \times 10^{15})h^{-1} M_\odot$. For $b = 0.15$ and $b = 0.3$, this effect is similar. These results are in good agreement with the results obtained by Sheth & Diaferio (2001). They studied the rms velocities of clusters in different mass intervals and found that the rms cluster velocity decreases with mass.

We also studied the rms velocity of clusters with density (or mass) higher than a given threshold density (or mass). The results are presented in Fig. 4. The DENS MAX clusters were ranked according to their density, and we selected $N_{cl} = (L/d_{cl})^3$ highest ranked clusters to produce cluster catalogues with a mean intercluster separation $10 - 50h^{-1} \text{ Mpc}$. Similarly, the FOF clusters were ranked according to their mass. Table 2 shows the density and mass thresholds used to produce cluster catalogues for different values of the mean cluster separation. For comparison, the number density of observed APM clusters and Abell clusters is $n_{cl} \sim 3.4 \times 10^{-5}h^3 \text{ Mpc}^{-3}$ ($d_{cl} \sim 31h^{-1} \text{ Mpc}$) and

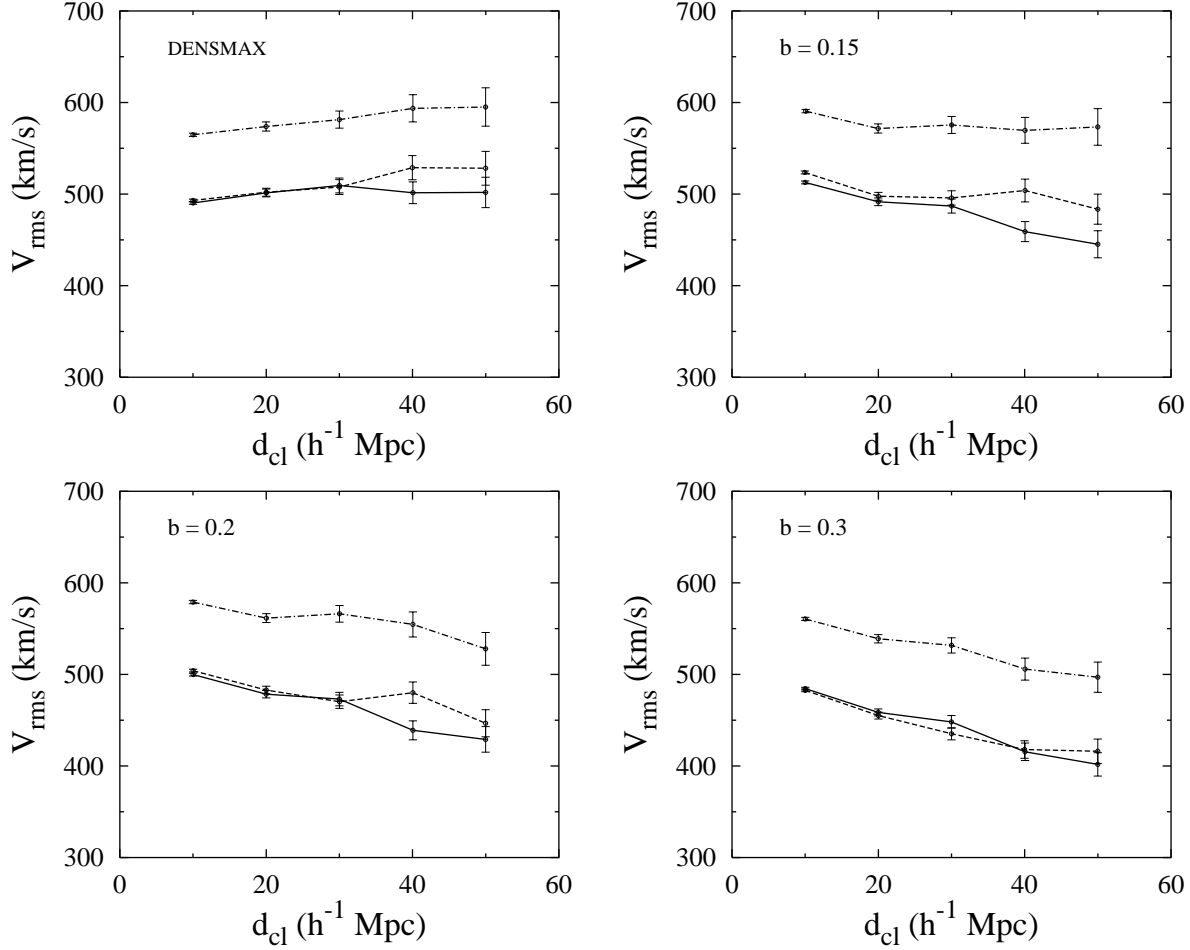


Figure 4. The rms peculiar velocities of clusters for different values of the mean cluster separation, d_{cl} . The clusters are ranked according to their density (DENSMAX clusters) or mass (FOF clusters). The lines are defined as in Fig. 3.

Table 2. The density and mass thresholds used to produce cluster catalogues with mean separations $d_{cl} = 10 - 50h^{-1}$ Mpc. The mass thresholds are given for the FOF clusters determined by $b = 0.2$.

d_{cl} (h^{-1} Mpc)	ρ_t/ρ_b Λ CDM1	ρ_t/ρ_b τ CDM	ρ_t/ρ_b Λ CDM2
10	35	27	20
20	213	102	136
30	435	178	264
40	652	254	393
50	850	315	505

d_{cl} (h^{-1} Mpc)	M_t (Λ CDM1) ($h^{-1} M_\odot$)	M_t (τ CDM) ($h^{-1} M_\odot$)	M_t (Λ CDM2) ($h^{-1} M_\odot$)
10	5.6×10^{12}	1.3×10^{13}	2.3×10^{12}
20	4.3×10^{13}	6.4×10^{13}	3.6×10^{13}
30	1.1×10^{14}	1.3×10^{14}	1.1×10^{14}
40	2.0×10^{14}	2.0×10^{14}	1.9×10^{14}
50	3.0×10^{14}	2.8×10^{14}	2.8×10^{14}

$n_{cl} \sim 2.5 \times 10^{-5} h^3 \text{ Mpc}^{-3}$ ($d_{cl} \sim 34 h^{-1} \text{ Mpc}$), respectively (Dalton et al. 1994, Einasto et al. 1997).

Fig. 4 demonstrates the rms peculiar velocity of clus-

ters with a mean separation $d_{cl} = 10 - 50 h^{-1} \text{ Mpc}$. In this range, the rms velocity of DENSMAX clusters is almost independent of the density of clusters. For the clusters with a mean separation $d_{cl} = 30 h^{-1} \text{ Mpc}$, $v_{rms} = 510 \text{ km s}^{-1}$ and $v_{rms} = 580 \text{ km s}^{-1}$ in the Λ CDM1 and τ CDM models, respectively. These values are similar to the linear rms velocity of peaks at the radius $R \sim 1 h^{-1} \text{ Mpc}$.

The rms velocity of FOF clusters decreases with cluster richness. For rich clusters, the rms velocity of FOF clusters is smaller than the rms velocity of clusters determined with the DENSMAX method. In the Λ CDM model for $b = 0.2$, the rms velocities are 500 km s^{-1} and 430 km s^{-1} , if $d_{cl} = 10 h^{-1} \text{ Mpc}$ and $d_{cl} = 50 h^{-1} \text{ Mpc}$, respectively. For $b = 0.15$ and $b = 0.3$, this effect is similar. For the clusters with $d_{cl} = 30 h^{-1}$ and $b = 0.2$, $v_{rms} = 475 \text{ km s}^{-1}$ and $v_{rms} = 565 \text{ km s}^{-1}$ in the Λ CDM1 and τ CDM models, respectively.

In Table 3 we compare the rms velocity of FOF clusters, v_{rms} , with $\sigma_p(R)$ for the radius $R = 1 h^{-1} \text{ Mpc}$. We analyzed the rms velocity of clusters for different values of the cluster separation. The results are given for the clusters determined by $b = 0.2$. The rms peculiar velocities v_{rms} for the clusters determined by $b = 0.15$ and $b = 0.3$ are similar. In the Λ CDM1 model, the rms peculiar velocity of small clusters is close to the linear theory expectations, while the rms pe-

Table 3. Comparison of the rms velocity of FOF clusters, v_{rms} , with the linear theory predictions for peculiar velocities of peaks, σ_p , for the radius $R = 1h^{-1}$ Mpc. The results are given for the FOF clusters determined by $b = 0.2$.

d_{cl} (h^{-1} Mpc)	v_{rms}/σ_p Λ CDM1	v_{rms}/σ_p τ CDM	v_{rms}/σ_p Λ CDM2
10	0.98	1.03	0.99
30	0.93	1.01	0.92
50	0.84	0.94	0.88

culiar velocity of rich clusters is smaller ($\approx 15\%$ per cent for clusters with a mean intercluster separation $d_{cl} = 50h^{-1}$ Mpc).

Our results are in good agreement with the results obtained by Colberg et al. (2000). They also studied the rms velocity of clusters in the Virgo Λ CDM and τ CDM models, but used a slightly different method to select clusters. High-density regions were located using a FOF method with $b = 0.05$ and their barycentres were considered as candidate cluster centers. Any candidate centre for which mass within $1.5h^{-1}$ Mpc exceeded the threshold mass M_t was identified as a candidate cluster. The final cluster list was obtained by deleting the lower mass candidate in all pairs separated by less than $1.5h^{-1}$ Mpc. The peculiar velocity of each cluster was defined to be the mean peculiar velocity of all the particles within the $1.5h^{-1}$ Mpc sphere. In this method, the size of the selected clusters is same for all clusters and in this sense, this method is similar to the DENS MAX method.

Colberg et al. (2000) used the value $M_t = 3.5 \times 10^{14}h^{-1}M_\odot$. For this value, the number of clusters was ≈ 70 in the Λ CDM1 and τ CDM models ($d_{cl} \approx 58h^{-1}$ Mpc). They found that the rms cluster velocities derived from simulation, v_s are 439 km s^{-1} and 535 km s^{-1} in the Λ CDM1 and τ CDM models, respectively (they did not include the dispersion v_L^2). If we use the DENS MAX method, we find that the rms velocity of clusters is almost independent of the number density of clusters and for $d_{cl} = 50h^{-1}$ Mpc, the velocities are $v_s = 450 \text{ km s}^{-1}$ and 549 km s^{-1} in the Λ CDM1 and τ CDM models, respectively. These values are very close to the values found by Colberg et al. (2000), only slightly larger (≈ 2 per cent). This small difference is probably caused by the fact that in the DENS MAX method we use the smoothing length $\sim 1h^{-1}$ Mpc, which is smaller than $1.5h^{-1}$ Mpc used by Colberg et al. (2000). For comparison, the rms velocities v_s for the FOF clusters for $b = 0.2$ and $d_{cl} = 50h^{-1}$ Mpc, are 368 km s^{-1} and 468 km s^{-1} in the Λ CDM and τ CDM models, respectively.

Let us now consider the rms velocities of clusters for different cluster radii. We studied the rms velocity of clusters with the effective radius R_{eff} larger than a given threshold radius. The clusters were ranked according to their effective radius and we selected $N_{cl} = (L/d_{cl})^3$ highest ranked clusters to produce cluster catalogues with mean separations $10 - 50h^{-1}$ Mpc. Table 4 shows the threshold radii used for different values of the mean cluster separation.

Fig. 5 illustrates the dependence of v_{rms} on cluster radii. We see that the effect of the cluster radius on v_{rms} is similar to the effect of the cluster mass on v_{rms} (compare Fig. 4 and Fig. 5). In the models studied, the rms velocity of small clusters is higher than the rms velocity of large clusters. For

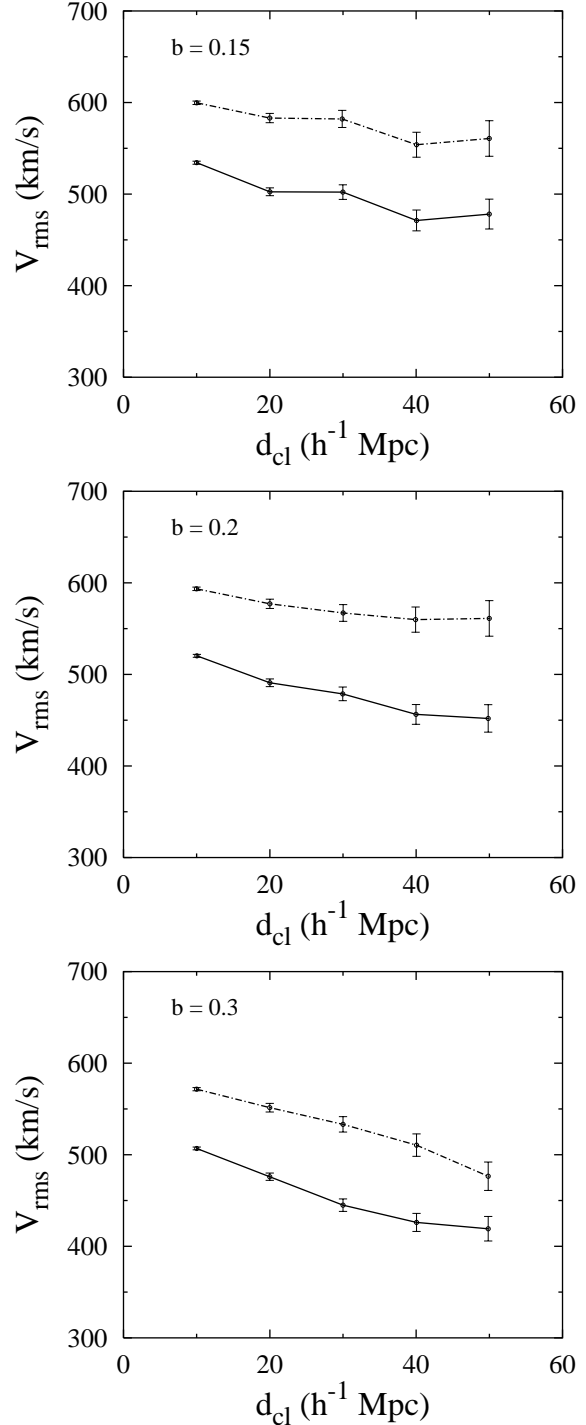


Figure 5. The rms peculiar velocities of clusters for different values of the mean cluster separation, d_{cl} . The clusters are ranked according to their effective radius, R_{eff} . The solid lines show the rms velocities in the Λ CDM1 model and the dot-dashed lines in the τ CDM model. The upper panel shows the velocities for the clusters defined by $b = 0.15$, the middle panel for the clusters defined by $b = 0.2$ and lower panel for the clusters defined by $b = 0.3$.

Table 4. The threshold radii R_t used to produce cluster catalogues with mean separations $d_{cl} = 10 - 50h^{-1}$ Mpc. The radii are given for the FOF clusters defined by $b = 0.2$.

d_{cl} (h^{-1} Mpc)	R_t (Λ CDM1) (h^{-1} Mpc)	R_t (τ CDM) (h^{-1} Mpc)
10	0.22	0.24
20	0.40	0.40
30	0.58	0.53
40	0.74	0.64
50	0.88	0.72

example, in the Λ CDM1 model for $b = 0.2$, the rms velocities are 520 km s^{-1} and 450 km s^{-1} for clusters with $d_{cl} = 10h^{-1}$ Mpc and $d_{cl} = 50h^{-1}$ Mpc, respectively.

4 THE SHIFTED-MESH SCHEME

When we started the study of cluster velocities we first used a PM code with a shifted-mesh scheme. In this scheme, the acceleration on the grid was calculated by using the approximation

$$g_x(i + \frac{1}{2}, j, k) = \varphi(i, j, k) - \varphi(i + 1, j, k), \quad (13)$$

where $\varphi(i, j, k)$ is the gravitational potential on the grid. A similar scheme for one-dimensional systems was proposed by Melott (1986). The traditional two-point finite-difference approximation for the acceleration is given by

$$g_x(i, j, k) = \frac{\varphi(i - 1, j, k) - \varphi(i + 1, j, k)}{2}. \quad (14)$$

Gramann (1987) studied the evolution of an one-dimensional plane-wave perturbation by using a PM code with differential operators (13) and (14) and found that the approximation (13) leads to smaller deviations from the exact solution than the approximation (14).

Fig. 6 shows the rms peculiar velocities of clusters in a PM simulation, where we used the approximation (13) for a three-dimensional system. The cosmological parameters in this simulation were chosen similar to the Λ CDM1 and Λ CDM2 models. We investigated the evolution of 256^3 particles on a 256^3 grid in the comoving box of size $L = 239.5h^{-1}$ Mpc. For comparison we show the rms peculiar velocities in the Λ CDM2 model with a standard finite-difference approximation (14). The clusters are defined by the FOF method with $b = 0.2$. The rms cluster velocities in the Λ CDM2 model are similar to the Λ CDM1 model, which achieves a force resolution smaller than the mean particle separation λ_p (see Fig. 3 and Fig. 4).

We see that the shifted-mesh scheme artificially boosts cluster velocities. The effect is particularly strong for rich clusters. The rms velocities are 560 km s^{-1} and 735 km s^{-1} , if $d_{cl} = 10h^{-1}$ Mpc and $d_{cl} = 50h^{-1}$ Mpc, respectively. This effect is probably caused by the fact that using the scheme (13), we calculate the components (g_x, g_y, g_z) at different locations on the grid and this can lead to artificial enhancement of particle acceleration in one dimension. This effect does not arise in an one-dimensional system, where $g_y = g_z = 0$.

In the Λ CDM2 model we used the standard two-point

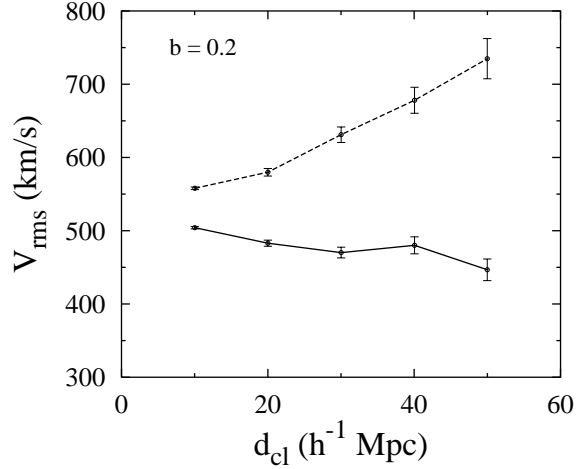


Figure 6. The rms peculiar velocities of clusters in the PM simulation, where we used the shifted-mesh scheme (13) (dashed line) and in the Λ CDM2 model using a standard approximation (14) (solid line)

finite-difference approximation (14). In this model, the rms velocities of clusters are similar to the Λ CDM1 model. Therefore, we can use the PM code to study peculiar velocities on scales that are close to the mean particle separation and force resolution. But it is important to use a correct difference operator in simulations.

5 SUMMARY AND DISCUSSION

In this paper we have examined the rms peculiar velocities of galaxy clusters, v_{rms} , for different cluster masses and radii. We analyzed clusters in the Virgo simulations for two cosmological models, Λ CDM and τ CDM (Jenkins et al. 1998). These simulations were carried out using the AP³M code. We used the simulations where the mean particle separation $\lambda_p \sim 1h^{-1}$ Mpc. We also analyzed clusters in an N-body simulation where the evolution was followed using a PM code with the same mass resolution that was used in the Virgo simulations. The cosmological parameters for this simulation were chosen similar to the Virgo Λ CDM model. We found that the rms velocities of clusters in the PM simulation are similar to the rms velocities in the AP³M simulation. We can use the PM code to study peculiar velocities on scales that are close to the mean particle separation λ_p .

To identify clusters in the simulations we used two methods: the standard friends-of-friends (FOF) method and the method where the clusters are defined as maxima of the density field smoothed on the scale $R \sim 1h^{-1}$ Mpc (DENSMAX). The velocity of DENSMAX clusters was determined using the same smoothing scale as for the density field. If we use the DENSMAX method, the size of the selected clusters is similar for all clusters. The velocity of FOF clusters was defined to be the mean velocity of all the particles in the cluster. If we use the FOF method, the size of the high-mass clusters is larger than the size of the low-mass clusters. We studied the velocities of FOF clusters defined by the parameters $b = 0.15$, $b = 0.2$ and $b = 0.3$ (the parameter b defines the linking length as $b\lambda_p$).

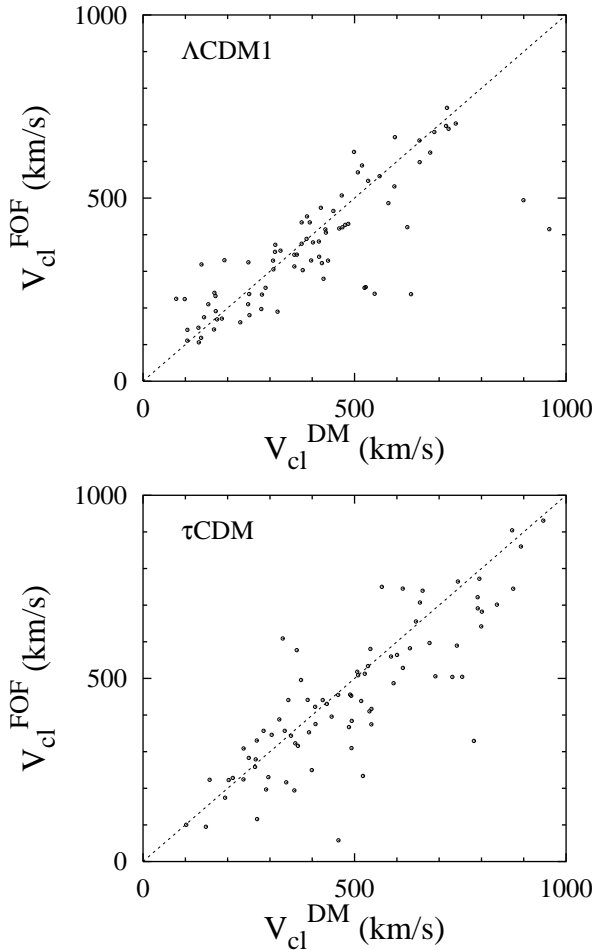


Figure 7. The cluster peculiar velocity defined using the DENS MAX method vs the cluster peculiar velocity defined by the FOF method. We show the velocities for rich clusters for $d_{cl} = 50h^{-1}$ Mpc. The upper panel shows the velocities in the Λ CDM model and the lower panel in the τ CDM model.

We found that the rms velocity of clusters defined with the DENS MAX method is almost independent of the density of clusters. The rms velocity of FOF clusters decreases with the cluster mass and radius. The effect of the cluster radius on v_{rms} is similar to the effect of the cluster mass on v_{rms} (see Fig. 4 and Fig. 5). The rms velocity of small clusters is higher than the rms velocity of large massive clusters. For different values of b , this effect is similar. In the Λ CDM model, the rms peculiar velocity of massive clusters with an intercluster separation $d_{cl} = 50h^{-1}$ Mpc is $\approx 15\%$ smaller than the rms velocity of clusters with a separation $d_{cl} = 10h^{-1}$ Mpc.

The rms velocity of massive FOF clusters is smaller than the rms velocity of high-density clusters determined with the DENS MAX method. What is the reason for this difference? Do we select different objects by using different methods or do we define different velocities for the same clusters? We analyzed the fraction of DENS MAX clusters, F , which match FOF clusters (in terms of their positions). We studied the FOF clusters determined with $b = 0.2$. In the Λ CDM model, if we compared DENS MAX clusters for $d_{cl} = 50h^{-1}$ Mpc with the FOF clusters for $d_{cl} = 50h^{-1}$ Mpc,

we found that the fraction of matched clusters is $F = 0.72$. For $d_{cl} = 30h^{-1}$ Mpc in both methods, the fraction $F = 0.74$. In the τ CDM model, the fraction F was similar. We select the same objects by using different methods, but we rank them in a somewhat different way. In the DENS MAX method, the clusters are ranked according to their density and in the FOF method according to their mass. If we compared DENS MAX clusters for $d_{cl} = 50h^{-1}$ Mpc with the FOF clusters for $d_{cl} = 40h^{-1}$ Mpc, we found that $F = 0.98$.

But we do assign different velocities for the same clusters by using different methods. Fig. 7 shows the peculiar velocities determined with different methods for the same clusters. We show the velocities of rich clusters that match for $d_{cl} = 50h^{-1}$ Mpc in both methods. We see that the velocities of clusters defined by the FOF method are systematically smaller than the velocities of clusters defined by the DENS MAX method. This is probably caused by the fact that in the FOF method, the size of rich clusters is larger than the smoothing scale $R \sim 1h^{-1}$ Mpc that was used to define the cluster velocities in the DENS MAX method.

We compared the rms velocities of clusters with the linear theory predictions for the rms peculiar velocities of peaks, σ_p , for the smoothing radius $R = 1h^{-1}$ Mpc. At this radius, $\sigma_p = 509 \text{ km s}^{-1}$ and $\sigma_p = 562 \text{ km s}^{-1}$ in the Λ CDM and τ CDM models, respectively. We analyzed the rms velocity of FOF clusters for different values of the cluster separation. In the Λ CDM model, the rms peculiar velocity of small clusters is close to the linear theory expectations, while the rms peculiar velocity of rich clusters is smaller (≈ 15 per cent for clusters with a mean separation $d_{cl} = 50h^{-1}$ Mpc). The rms velocity of DENS MAX clusters is almost independent of the cluster density and is similar to the linear theory expectations. For the DENS MAX clusters with a mean separation $d_{cl} = 30h^{-1}$ Mpc, $v_{rms} = 510 \text{ km s}^{-1}$ and $v_{rms} = 580 \text{ km s}^{-1}$ in the Λ CDM and τ CDM models, respectively. On scales probed by galaxy clusters, velocity fluctuations are in the quasi-linear regime.

ACKNOWLEDGEMENTS

We thank J. Einasto, M. Einasto, P. Heinämäki, G. Hützi, A. Melott and E. Saar for useful discussions. This work has been supported by the ESF grant 3601. The N-body simulations used in this paper are available at <http://www.mpa-garching.mpg.de/Virgo/virgoproject.html>. These simulations were carried out at the Computer Center of the Max-Planck Society in Garching and at the EPCC in Edinburgh, as part of the Virgo Consortium project. The FOF programs used in this paper are available at <http://www-hpcc.astro.washington.edu>. These programs were developed in the University of Washington.

REFERENCES

Aghanim N., Gorski K.M., Puget J.L., 2001, A&A, 374, 1
Bahcall N.A., Gramann M., Cen R. 1994, ApJ, 436, 23
Bahcall N.A., Oh S.P. 1996, ApJ, 462, L49
Bardeen J.M., Bond J.R., Kaiser N., Szalay A.S. 1986, ApJ, 304, 15
Bond J.R., Efstathiou G., 1984, ApJ, 285, L45

Borgani S., da Costa L.N., Freudling W., Giovanelli R., Haynes M.P., Salzer, J., Wegner, G. 1997, ApJ, 482, L121

Borgani S., Bernardi M., da Costa L.N., Wegner G., Alonso M.V., Willmer C.N.A., Pellegrini P.S., Maia M.A.G., 2000, ApJ, 537, L1

Colless M., Saglia R.P., Burstein D., Davies R.L., McMahan R.K., Wegner G., 2001, MNRAS, 321, 277

Colberg J.M., White S.D.M., MacFarland T.J., Jenkins A., Pearce F.R., Frenk, C.S., Thomas P.A., Couchman H.M.P., 2000, MNRAS, 313, 229

Croft R.A.C., Efstathiou G., 1994, MNRAS, 268, L23

Couchman H.M.P., Thomas P.A., Pearce F.R., 1995, ApJ, 452, 797

Dale D.A., Giovanelli R., Haynes M.P., Campusano L.E., Hardy E. 1999, AJ, 118, 1489

Dalton, G.B., Croft, R.A.C., Efstathiou, G., Sutherland, W.J., Maddox, S.J., Davis, M. 1994, MNRAS, 271, L47

Diego J., Hansen S. & Silk J. 2002, MNRAS, submitted, astro-ph: 0207178

Efstathiou G., Davis M., Frenk C.S., White S.D.M., 1985, ApJS, 57, 241

Einasto, J., et al. 1997, Nature, 385, 139

Giovanelli R., Haynes M.P., Herter T., Vogt N.P., Wegner G., Salzer J.J., da Costa L.N., Freudling W., 1997, AJ, 113, 22

Gramann M., 1987, Tartu Obs. Publ., 52, 216

Gramann M., 1988, MNRAS, 234, 569

Götz M., Huchra J.P., Brandenberger R.H., astro-ph:9811393

Haehnelt M.G., Tegmark M., 1996, MNRAS, 279, 545

Hockney R.W. & Eastwood J.W., 1981, Numerical simulations using particles (New York: McGraw-Hill)

Holder G.P., 2002, astro-ph: 0207600

Holzapfel W.L., Ade P.A.R., Church S.E., Mauskopf P.D., Rephaeli Y., Wilbanks T.M., Lange A.E., 1997, ApJ, 481, 35

Hudson M.J., Smith R.J., Lucey J.R., Schlegel D.J., Davies R.L., 1999, ApJ, 512, L79

Jenkins A. et al. (The Virgo Consortium), 1998, ApJ, 499, 20

Jenkins A., Frenk C.S., White S.D.M., Colberg J.M., Cole S., Evrard A.E., Couchman H.M.P., Yoshida N., 2001, MNRAS, 321, 372

Lamarre J.M. et al., 1998, ApJ, 507, L5

Lauer T.R., Postman M. 1994, ApJ, 425, 418

Melott A.L. 1986, Phys. Rev. Lett., 56, 1992

Moscardini L., Branchini E., Brunozi P.T., Borgani S., Plionis M., Coles P. 1996, MNRAS, 282, 384

Nagai D., Kravtsov A.V., Kosowsky A., 2002, ApJ submitted, astro-ph: 0208308

Pearce F.R., Couchman H.M.P., 1997, NewA, 2, 411

Rephaeli Y., Lahav O. 1991, ApJ, 372, 21

Sheth R.K., Diaferio A., 2001, MNRAS, 322, 901

Suhhonenko I., Gramann M., 1999, MNRAS, 303, 77

Sunyaev R.A., Zel'dovich Y.B., 1980, MNRAS, 190, 413

Watkins R. 1997, MNRAS, 292, L59

Willlick J.A., Courteau S., Faber S.M., Burstein D., Dekel A., Strauss M.A., 1997, ApJS, 109, 333